

Fluid Jet and Bonnet Polishing of Optical Moulds for Application from Visible to X-Ray

Anthony T. H. Beaucamp^{*a,b}, Richard R. Freeman^a, Akihiro Matsumoto^b, Yoshiharu Namba^b

^aZeeko Ltd, Vulcan Court, Coalville, Leicestershire, LE67 3FW, United Kingdom

^bDept. of Mechanical Engineering, Chubu University, Kasugai, 487-8501, Japan

ABSTRACT

Electroless Nickel (ENi) and binderless Tungsten Carbide (WC) are materials widely used in industry to make replication moulds for precision optics, with applications ranging from consumer camera lenses to high accuracy X-ray mirrors. The aspheric shape generation is generally performed by diamond turning in the case of Nickel, and micro-grinding in the case of Tungsten Carbide. However, both machining methods fall short from meeting the ultra-precision criteria required by an increasing number of applications, because of insufficient form accuracy and the frequency content of the machining marks they leave on the surface. It is thus commonly observed in industry that moulds need to be subsequently polished by hand, a usually slow and human resource intensive operation. The Zeeko 7-axis CNC machine, equipped with sub-aperture fluid jet and precessed bonnet polishing technology, has been used to develop deterministic finishing processes on both Electroless Nickel and Tungsten Carbide. Corrective polishing to less than $\lambda/20$ ($<31\text{nm PV}$) form error can be achieved, as well as the ability to smooth surface texture down to 1nm Ra or less, in a time efficient manner.

Keywords: Ultra-Precision, Finishing, Optical Moulds, Carbide, Nickel

1. INTRODUCTION

Because of the increasing demand for low-cost and high-accuracy optical systems in consumer products such as digital cameras, the preferred manufacturing method of many optical components is quickly evolving from direct glass generation to glass press moulding. Moulds are often made from a ceramic material such as binderless tungsten carbide. The aspheric or freeform shape generation into the mould is usually performed by grinding with resinoid bonded diamond wheels¹⁻³. In the case of higher accuracy or larger size optical components, Electroless Nickel may be used instead and machined by diamond turning. However, both of these generation methods results in cyclic micro-structures that may cause diffraction and stray light effects.

Some finishing techniques have already been developed to address this issue: ultrasonic two-axis vibration assisted polishing⁴⁻⁵ has been shown to achieve ultra precision accuracy finishing on high numerical aperture moulds below 5 mm diameter, but the polishing of larger moulds up-to 50 mm diameter by this technique would take an excessively long time; in the conventional aspheric polishing method, a soft polishing tool is contacting normal to the surface and rotated while loose abrasives are supplied, but the high hardness of tungsten carbide also makes this method exceedingly slow⁶⁻⁸. For these reasons, a large number of optical moulds manufacturers are still relying on hand polishing, a notoriously human resource intensive operation, to finish the moulds after micro-grinding.

Namba et.al have previously described their work on replication-mandrels for Wolter Type 1 mirrors used in soft X-ray microscopy⁹ and hard X-ray telescopes¹⁰. The electroless nickel plated mandrels were produced by single-point diamond turning, but required post-polishing by hand to remove the high spatial frequencies on the surface. As they pointed out, this is extremely difficult on aspheres, and leads to an inevitable trade-off between quality of the surface texture achieved and destruction of the aspheric figure.

There is thus a need for a fully automated and time-efficient finishing method capable of achieving ultra-precision accuracy on moulds up-to 100 mm in diameter while removing the signature from either diamond or micro-grinding operations. PrecessionsTM, an innovative CNC process based on precessed bonnet and fluid jet polishing, is presented in this paper together with the latest developments in the polishing of optical moulds. The process has been described previously in the literature at various stages of its development¹¹⁻¹². An overview of the precessed bonnet and fluid jet polishing technologies is provided in the following sections.

1.1 Precessed Bonnet Polishing

The position and orientation (precession angle) of a spinning, inflated, membrane-tool are actively controlled as it traverses the surface of a workpiece. The workpiece may have any general shape, including flat, concave or convex, aspheric or free-form. While a classical polishing tool is pressurized against the surface of the part, with no attempt to control actively the Z position of the tool in a local or global coordinate frame, in the technique we describe the Z position and precession (but not directly the contact-force) are actively controlled with a CNC machine tool.

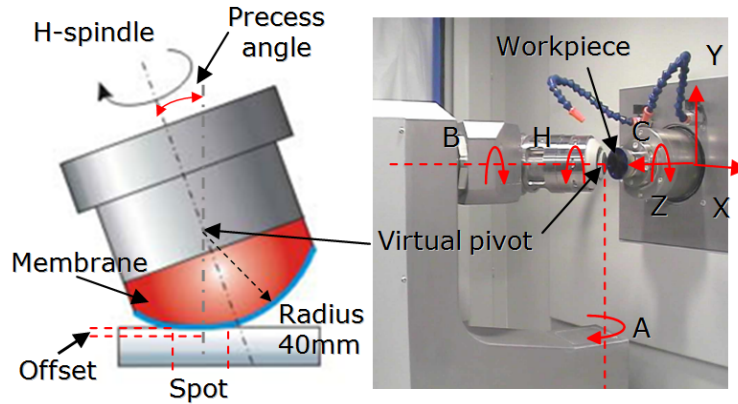


Figure 1. Principle of precessed polishing tool and 7-Axis CNC machine.

Fig. 1 shows the seven CNC-controlled axes available on the Zeeko polishing machine: three axes of translation (X, Y, Z), two axes of rotation intersecting at a virtual pivot point (A, B), and two rotation spindles (H, C). It is possible to numerically control the precess angle, spindle speed, geometrical offset, and surface feed of the polishing spot to obtain variations in spot size and removal rate. The bonnet tool can be manufactured in a range of sizes from 0.5mm to 320mm, according to the workpiece size and curvature.

1.2 Fluid Jet Polishing

Fluid-jet polishing (FJP) is a method in which slurry of polishing particles is pressurized and projected through a nozzle towards the surface to be polished. The jet impacts the surface of the part directly, i.e. with no physical tool contact. Booij et.al¹³ have shown the linear dependence of removal rate with slurry concentration. They have also shown the non-linear dependence with impact-velocity, due to the combined effects of i) a minimum velocity-threshold below which no removal occurs, ii) the increased rate of particle-delivery with increased velocity and iii) the square relation between particle kinetic energy and velocity. They conclude that, using appropriate abrasive and particle size with the right flow velocity, FJP can achieve ductile-regime removal with stable volumetric removal-rate. L. Yang et.al have also investigated fluid jet polishing and concluded¹⁴ that the removal process is a mixture of shear and collision mechanisms. The FJP process parameters include: nozzle diameter, fluid pressure, abrasive type and concentration, stand-off distance from the work surface, angle of impingement of the jet.

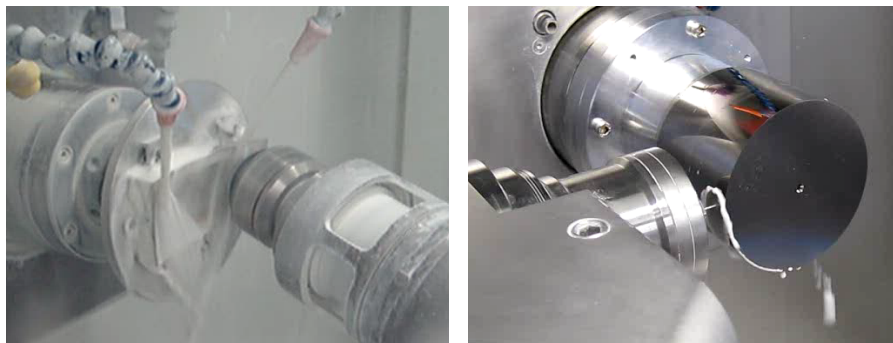


Figure 2. Examples of Bonnet (left) and Fluid Jet (right) polishing operations on the Zeeko 7-Axis CNC machine.

2. APPLICATION TO TUNGSTEN CARBIDE (WC)

The preprocessed polishing tool normally consists of an inflated reinforced rubber membrane onto which a cloth or pad is stuck. This pressurized membrane has been used to achieve stable geometrical sphericity of the bonnet when the tool radius is 20 mm and above¹⁻². For miniaturization to smaller radii, the tool can be simplified to a stem onto which a thick polyurethane pad is firmly bonded (see Fig. 3a).

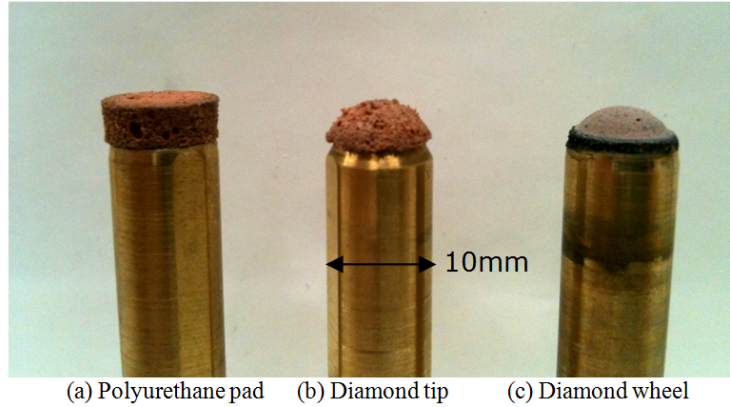


Figure 3. Miniaturized polishing tool at successive preparation stages.

2.1 On-Machine Tool Forming

The cloth is cut to a spherical shape on-machine, by a diamond tip placed in the C-axis chuck holder. By moving the A-axis back and forth at low speed (5 deg/min) and spinning the H-axis spindle (1000 rpm), a sphere of known radius and centered on the virtual pivot point intersecting the A and B-axis is generated into the rigid polyurethane cloth (see Fig 3b). The CNC machine is equipped with a load cell sensor on the H-axis spindle, so it is possible to check run-out errors on the nominal sphere shape obtained from the dressing operation. A tool was precessed at 20 deg angle and probed for a range of angles of the H-axis. It was found that cloth plucking by the diamond tip can cause large amounts of run-out error (Fig. 4 blue curve).

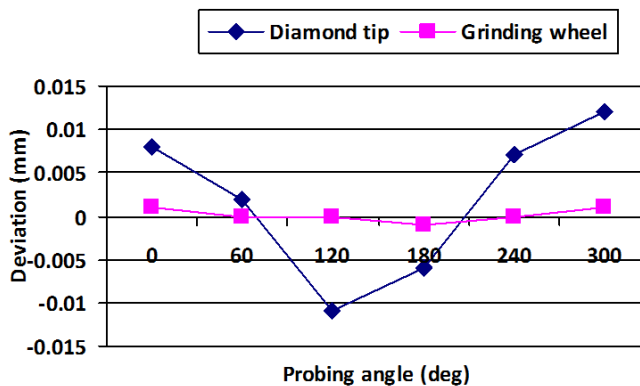


Figure 4. Deviation from nominal sphere at 20 deg precess angle.

A second dressing step is performed on the polishing tool by spinning a grinding wheel in the C-axis at 750 rpm while repeating the same motion as previously with the A and H-axis (see Fig. 4). It is thus possible to smooth the surface of the tool, and reduce run-out errors to less than 3 μm (see Fig. 3c and Fig. 4 pink curve). This reduction in run-out errors is essential, as it reduces significantly waviness from the polishing performance of the precessed tool.

2.2 Surface Texture Performance

Plano WC samples of 25 mm diameter were generated with a grinding wheel moving at an angle across the spinning surface, to replicate aspheric mode grinding conditions. By using this method, surface roughness between 8-9 nm Ra was obtained across the batch of samples. A series of experiments was then conducted to assess the performance of the polishing tool for a range of diamond abrasives. The process parameters shown in Table 1 were used for the experiments. Mono-crystalline diamond abrasives of grit sizes 3.0, 1.0 and 0.25 μm in an oily suspension were fed with a peristaltic pump above the polishing tool, while it moved across the surface in a raster tool-path.

Table 1. Process parameters for surface texture experiments.

Workpiece	Binderless tungsten carbide Grain size: 0.2 μm
Polishing tool Radius Shore hardness	Polyurethane 4.5 mm 90 A
Tool-path mode Point spacing Tool offset Head speed Precess angle Surface feed	Raster 0.25 mm 0.1 mm 2000 rpm 20 deg 500 mm/min
Abrasives Grain size Density	Mono-crystalline diamond 0.25; 1.0; 3.0 μm 1 wt %

Removals were measured with a 3D optical profiler. A wide range of removal rates was observed for the various grit sizes, from 0.002 mm^3/min to 0.039 mm^3/min (Fig. 5a). On the 25 mm diameter workpiece, with the chosen parameters a uniform 200 nm layer of material could be removed in 10 min using the 3.0 μm abrasive, and in 40 min using the 1.0 μm abrasive. Because removals follow a square law of the spot size, these results show that polishing of WC by this method is time efficient. In each case, surface texture measurements with a white-light interferometer showed that the grinding marks were successfully removed from the surface after the polishing of a 200 nm layer of material. Surface texture down to 1.6 nm Ra was achieved with the smallest 0.25 μm grit size (see Fig. 5b).

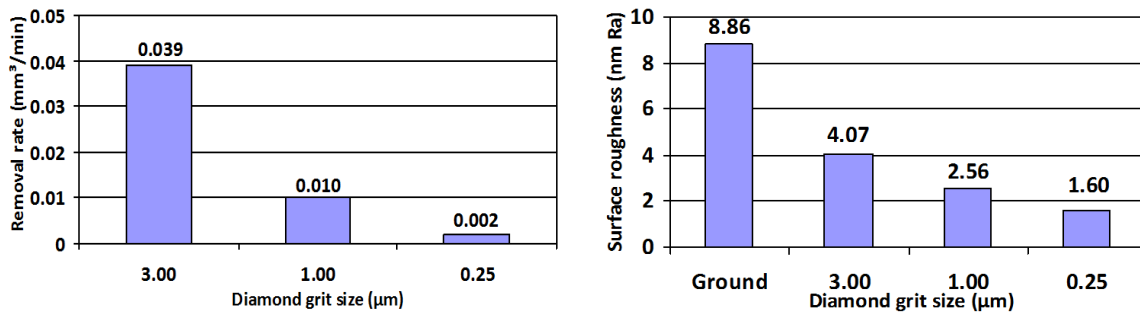


Figure 5. Removal rates (a) and surface roughness (b) observed for various diamond grit sizes.

Fig. 6 shows the optimal surface texture attainable for each grit size. The resulting surface texture contains some residual waviness, the overall amplitude of which was observed to decrease in the spectral domain as the grit size became smaller. It was also found that a surface first polished with the 3.0 μm grit diamond needs only 100 nm of extra removals with the 1.0 μm grit diamond to bring roughness down to circa Ra 2.5 nm. Similarly, a surface first polished with the 1.0 μm grit diamond needs only 50 nm of extra removals with the 0.25 μm grit diamond to bring roughness down to circa

1.6 nm Ra. These results indicate that a multiple step process, including form correction with the larger grit, and surface texture smoothing with the smaller grit, can be deployed. Combinations of the 3.0 μm , 1.0 μm and 0.25 μm abrasives can be used, depending on the required polishing time and final surface texture specification. The use of a peristaltic pump with removable tubing, and a rubber containment unit around the polishing area, made the transition between grit sizes fast and convenient.

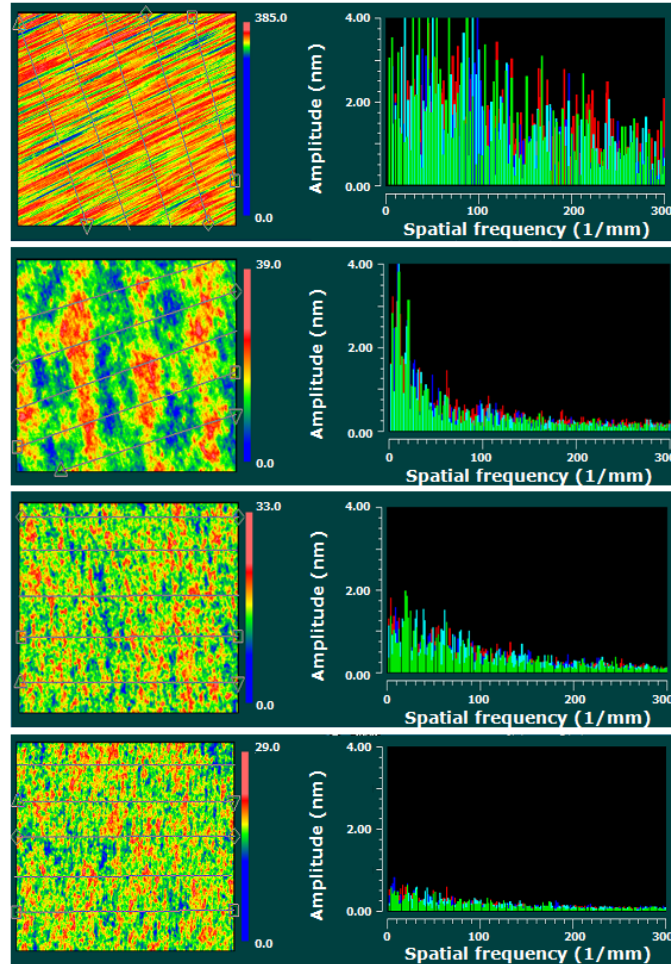


Figure 6. Surface texture and spectral analysis of WC surface under various conditions.
From top to bottom: ground, 3.0 μm , 1.0 μm , 0.25 μm diamond grit size.

Further experiments were conducted using optical polishing pitch. The miniaturized polishing tool was pressed by hand into a 1mm dollop of pitch warmed on a hot plate. After cooling, the edge of the pitch was trimmed with a cutting blade down to a disc of diameter around 2 mm. After mounting the tool inside the machine, the pitch was warmed repeatedly for short intervals of time with a small flame until it softened. The Z-axis was then moved forward to press the pitch tip of the tool against the workpiece, causing the pitch to conform to the surface curvature. Subsequent polishing was performed at 0 rpm H-axis speed, the pitch tool being simply dragged across the surface along a raster tool path at 500 mm/min. Polishing by this technique with 0.25 μm diamond abrasives consistently improved surface texture from 1.6 nm Ra down to 1.0 nm Ra.

2.3 Form Correction Performance

In order to test the performance of corrective polishing with reliable metrology at the $\lambda/20$ level of accuracy, a plano WC sample of diameter 25 mm was prepared by the same grinding method as described in section 2.2. The sample was measured with a laser interferometer which showed surface deviation from flat to be 905 nm Peak-to-Valley (P-V).

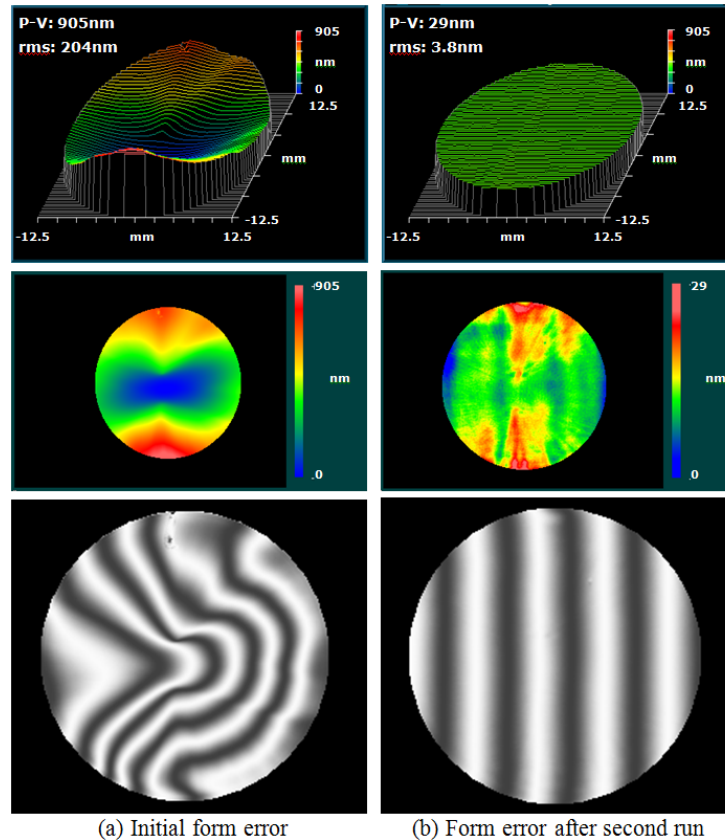


Figure 7. Comparison of form error before and after corrective polishing.

The PrecessionsTM Corrective polishing software was used to numerically optimize raster polishing tool paths on this sample. The software uses influence functions generated on a piece of same material and curvature to optimize the feed rate of the polishing spot across the workpiece. The first corrective polishing run used 1.0 μm diamond slurry and a spot size of 3 mm. Total polishing time was 23 min, and form error was reduced to 122 nm P-V. The second corrective polishing run used 0.25 μm diamond slurry and a spot size of 2 mm. Total polishing time was 25 min, and form error was reduced to 29 nm P-V. Initial and final form errors are shown side-by-side in Fig. 7. Interferometric fringes are also displayed, with the final state showing very straight and smooth fringes.

Both tooling and software used for this experiment are directly applicable to aspheres and freeforms. Both concave and convex aspheric moulds have been correctively polished by the same method down to a form error of less than 40nm P-V (which is the accuracy level of the 3D profilometer used in such case).

3. APPLICATION TO ELECTROLESS NICKEL (ENIP)

A7075 aluminum alloy was cut into 100mm diameter and 30 mm thick plano sample and turned by a single-point diamond turning machine. A layer of nickel-phosphorus alloy 0.1 mm thick was deposited on the diamond-turned aluminum alloy samples by electroless nickel plating. The hardness of the electroless nickel and aluminum alloy were 568 Hv and 183 Hv respectively. The plated sample was cut again on the single-point diamond turning machine. The form error was measured at 403nm P-V, and surface roughness at 3.05nm rms.

3.1 Fluid Jet Polishing

Using the PrecessionsTM software, the sample was polished by fluid jet with 200nm Al_2O_3 particles and 18Bar pressure, reducing the form error to 30nm P-V in two iterations (see fig. 8). Additionally, the diamond turning marks were removed from the surface (see Fig. 9a & 9b). This property of fluid jet polishing has been documented previously¹⁵.

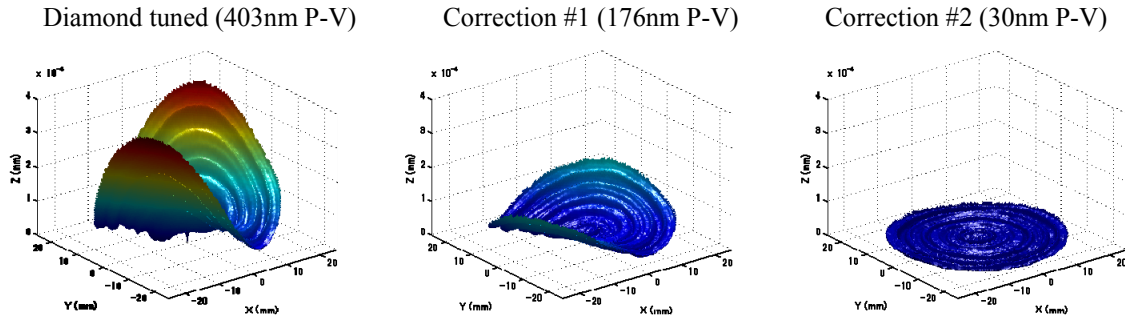


Figure 8. Iterative corrections from diamond turned state by fluid jet polishing.

3.2 Preprocessed Bonnet Polishing

After fluid jet polishing, a second polishing was performed with the preprocessed bonnet tool. A powder of ultra fine nano-particles with average size 30nm was mixed with pure water at a concentration of 20g/L. The slurry was delivered above the bonnet at a rate of 12L/H. To prevent drying of the slurry on the surface, which can cause crystallization, the surface was sprayed with a fine mist of pure water every few seconds. The slurry and water were thus delivered in total loss mode. Bonnet pressures in the range 0.2 to 3.0bar were experimented with, and the best pressure was found to be 1.0Bar.

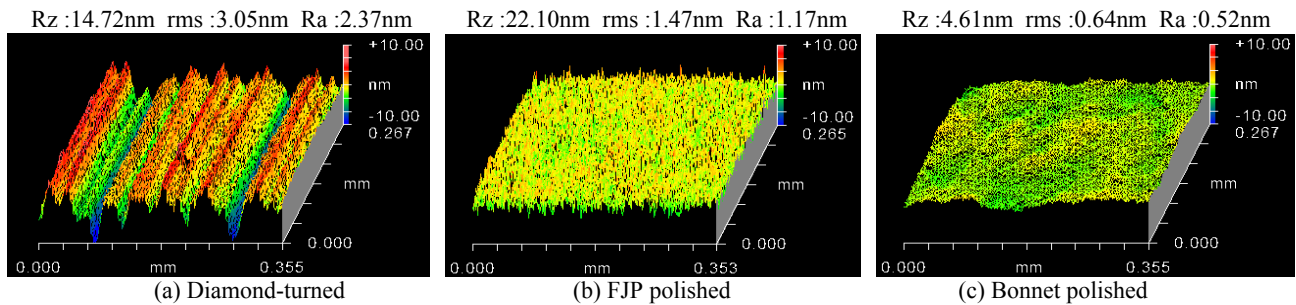


Figure 9: Surface texture of electroless nickel plano surface at various machining stages.

The surface texture was evaluated after a number of raster passes on the surface. Using filtering, the evolution of waviness (low-pass) and roughness (high-pass) could be assessed (see Fig. 10). The roughness component was quickly reduced to circa 0.3nm rms. Waviness was also reduced, albeit at a slower pace. Overall texture was reduced down to 0.64nm rms (Fig. 9c) after 5 raster passes.

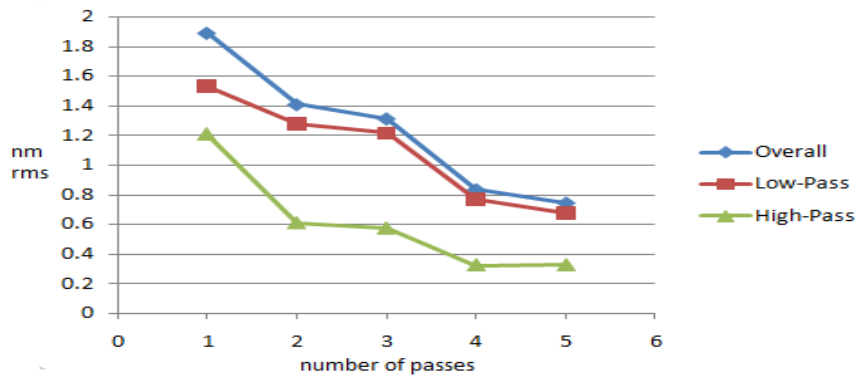


Figure 10: Surface texture improvement on ENiP sample, using bonnet polishing with nano-particles.

CONCLUSION

A need has been identified for an automated process capable of finishing aspheric and freeform optical moulds to ultra-precision criteria, in order to replace the hand polishing operation that is still commonly used at many industrial sites.

Finishing processes based on precessed bonnet and fluid jet polishing have been demonstrated on both Tungsten Carbide and Electroless Nickel. They can be used to finish optical moulds to a form error of less than $\lambda/20$ (<31nm PV) and surface texture of 1.0nm Ra or less.

Available on a common machine platform and applicable to materials most widely used for making optical moulds, these processes are already delivering substantial cost and time savings at industrial sites where they have been recently adopted.

REFERENCES

- [1] Semba, T., Tani, Y., Sato, H., "Development of Melanine-Bonded Diamond Wheels with High Porosity for Smooth and Mirror Finishing of Die Materials", *Annals of the CIRP*, 45/1, 315-318 (1996).
- [2] Chen, W., Kuriyagawa, T., Huang, H., Yosihara, N., "Machining of Micro Aspherical Mould Inserts", *Precision Engineering*, 29/3, 315-323 (2005).
- [3] Suzuki, H., Moriwaki, T., Yamamoto, Y., Goto, Y., "Precision Cutting of Aspherical Ceramic Molds with Micro PCD Tool", *Annals of the CIRP*, 56/1, 131-134 (2007).
- [4] Suzuki, H., Moriwaki, T., Okino, T., Ando, Y., "Development of Ultrasonic Vibration Assisted Polishing Machine for Micro Aspheric Die and Mold", *Annals of the CIRP*, 55/1, 385-388 (2006).
- [5] Suzuki, H., Hamada, S., Okino, T., Kondo, M., Yamagata, Y., Higuchi, T., "Ultraprecision Finishing of Micro Aspheric Surface by Ultrasonic Two-Axis Vibration Assisted Polishing", *Annals of the CIRP*, 59/1, 347-350 (2010).
- [6] Komanduri, R., Lucca, D.A., Tani, Y., "Technological Advances in Fine Abrasive Process", *Annals of the CIRP*, 46/2, 545-596 (1997).
- [7] Evans, C.J., Paul, E., Dornfeld, D., Lucca, D.A., Byrne, G., Tricard, M., Klocke, F., "Material Removal Mechanisms in Lapping and Polishing", *Annals of the CIRP*, 52/2, 611-633 (2003).
- [8] Brinksmeier, E., Riemer, O., Gessenharter, A., Autschbach, L., "Polishing of Structured Molds", *Annals of the CIRP*, 53/1, 247-250 (2004).
- [9] Chon, K. S., Namba, Y. and Yoon, K. H., "Precision Machining Electroless Nickel Mandrel and Fabrication of Replicated Mirrors for a Soft X-Ray Microscope", *JSME Int'l Journal Series C*, 49/1:56-62 (2006).
- [10] Y. Namba, T. Shimomura, A. Fushiki, A. Beaucamp, I. Inasaki, H. Kunieda, Y. Ogasaka, K. Yamashita, "Ultra-Precision Polishing of Electroless Nickel Molding Dies for Shorter Wavelength Applications", *Annals of the CIRP*, 57/1:337-340 (2008).
- [11] Walker, D., Brooks, D., King, A., Freeman, R., Morton, R., McCavana, G., Kim, S., "The Precessions Tooling for Polishing and Figuring Flat, Spherical and Aspheric Surfaces", *Optics Express*, 11/8, 958-964 (2003).
- [12] Walker, D., Freeman, R., Morton, R., McCavana, G., Beaucamp, A., "Use of the Precessions Process for Prepolishing and Correcting 2D and 2.5D Form", *Optics Express*, 14/24, 11787-11795 (2006).
- [13] Booj, S., Van Brug, H., Braat, J., Fahnle, O., "Nanometer Deep Shaping with Fluid Jet Polishing", *Opt Eng Vol. 41*, pp 1926-1931 (2002)
- [14] Guo, P., Fang, H., Yu, J., "Computer Controlled Fluid Jet Polishing", *Proc. SPIE*, Vol. 6722 (2007)
- [15] Beaucamp, A., Freeman, R., Morton, R., Ponudurai, K., Walker, D., "Removal of diamond-turning signatures on x-ray mandrels and metal optics by fluid-jet polishing", *Proc. SPIE*, Vol. 7018 (2008).